HEMATOPOIESIS

AIBP-mediated cholesterol efflux instructs hematopoietic stem and progenitor cell fate

Qilin Gu[1], Xiaojie Yang[1]*, Jie Lv[1,2]*, Jiaxiong Zhang[1,3]*, Bo Xia[1,2], Jun-dae Kim[1], Ruoyu Wang[4,5], Feng Xiong[4], Shu Meng[1], Thomas P. Clements[6], Bhavna Tandon[6], Daniel S. Wagner[6], Miguel F. Diaz[7], Pamela L. Wenzel[7], Yury I. Miller[8], David Traver[9], John P. Cooke[1,10,11], Wenbo Li[4,5], Leonard I. Zon[12], Kaifu Chen[1,2,10,11]†, Yongping Bai[3]†, Longhou Fang[1,10,11,13]†

Hypercholesterolemia, the driving force of atherosclerosis, accelerates the expansion and mobilization of hematopoietic stem and progenitor cells (HSPCs). The molecular determinants connecting hypercholesterolemia with hematopoiesis are unclear. Here, we report that a somite-derived prohematopoietic cue, AIBP, orchestrates HSPC emergence from the hemogenic endothelium, a type of specialized endothelium manifesting hematopoietic potential. Mechanistically, AIBP-mediated cholesterol efflux activates endothelial Srebp2, the master transcription factor for cholesterol biosynthesis, which in turn transactivates Notch and promotes HSPC emergence. Srebp2 inhibition impairs hypercholesterolemia-induced HSPC expansion. Srebp2 activation and Notch up-regulation are associated with HSPC expansion in hypercholesterolemic human subjects. Genome-wide chromatin immunoprecipitation followed by sequencing (ChIP-seq), RNA sequencing (RNA-seq), and assay for transposase-accessible chromatin using sequencing (ATAC-seq) indicate that Srebp2 transregulates Notch pathway genes required for hematopoiesis. Our studies outline an AIBP-regulated Srebp2-dependent paradigm for HSPC emergence in development and HPSC expansion in atherosclerotic cardiovascular disease.

Hematopoietic stem and progenitor cells (HSPCs) maintain hematopoietic output by generating the whole spectrum of blood cell lineages in vertebrate animals. Previous studies demonstrate that blood vessels play an essential role in HSPC specification in development (*1*–*4*). During embryogenesis, HSPCs emerge from a rare population of endothelial cells (ECs) residing on the floor of the dorsal aorta (DA) (*1*–*4*). Our earlier studies show that apoA-I binding protein 2 (Aibp2, also known as Yjefn3) regulates angiogenesis from the DA (*5*). Because hematopoietic stem cells (HSCs) arise from the ventral DA (*1*–*3*), we investigated the role of Aibp2 in hematopoiesis. We generated *apoa1bp2*$^{-/-}$ zebrafish (fig. S1, A to E), which appeared morphologically normal (fig. S2). The expression of HSC marker genes *runx1* and *cmyb* in the ventral DA and the expression of *rag1*, which marks HSC-derived T lymphocytes in the thymus, were substantially reduced in *apoa1bp2*$^{-/-}$ animals (Fig. 1A and fig. S3A). Aibp2 depletion had no observable effect on DA specification, as revealed by unaffected arterial *efnb2a* expression (*6*) (Fig. 1A). Morpholino antisense oligonucleotide–mediated Aibp2 knockdown (fig. S4, A and B) or antibody-mediated extracellular Aibp2 neutralization (fig. S4, C and D) reproduced the Aibp2 knockout effect on hematopoiesis. Consistently, Aibp2 deficiency reduced the number of *cmyb*$^{+}$*kdrl*$^{+}$ cells, which mark nascent HSCs in the ventral DA between 28 and 60 hours postfertilization (hpf) (Fig. 1B and fig. S3B). The results were validated by using fluorescence-activated cell sorting (FACS) analysis of *cmyb*$^{+}$*kdrl*$^{+}$ cells (fig. S3, C and D). Although blood flow regulates hematopoiesis (*7*), blood flow appeared normal in Aibp2-deficient *gata1:DsRed* zebrafish (movies S1 and 2). These data suggest that Aibp2 governs HSC ontogeny in a direct and non–cell autonomous fashion.

The expression of primitive hematopoiesis genes *gata-1* and *l-plastin* at 24 hpf was normal in *apoa1bp2* morphants, whereas the marker of HSC-derived leukocytes (*l-plastin*$^{+}$) was reduced at 4 days postfertilization (fig. S5). We also examined the integrity of nonhematopoietic tissues by surveying the expression of associated marker genes. Development of the pronephros (*cdh17*), somite (*desma*), and sclerotome (*nkx3.1*) in the trunk (fig. S6A); sonic hedgehog (shh) signaling (*shha* and *vegfa*); and arterial (*dll4*) and venous (*ephb4*) vasculature development showed no apparent changes in the absence of Aibp2 (fig. S6B). Pan-endothelial markers *fli1* and *kdrl* were increased in Aibp2-deficient animals (*5*). These results suggest that Aibp2 plays a direct role in HSC specification.

Our previous study showed increased cholesterol contents in Aibp2-deficient embryos (*5*). To determine the effect of cholesterol on HSC emergence, *apoa1bp2* knockouts or morphants were treated with a cholesterol-lowering drug, atorvastatin. Atorvastatin treatment largely restored *runx1* expression (Fig. 1C and fig. S7, A to E) and reduced free cholesterol levels in Aibp2-deficient animals (fig. S7, B and E). Furthermore, atorvastatin expanded the *cmyb*$^{+}$*kdrl*$^{+}$ cells in the DA floor (fig. S7, F and G). These results indicate that an effective cholesterol metabolism program orchestrates HSC emergence.

Cholesterol synthesis requires the master transcription factor Srebp2 (*8*), which is produced as an endoplasmic reticulum (ER)–bound precursor. Cholesterol depletion activates Srebp2 via two-step proteolytic cleavages, and Srebp2 then releases its N-terminal transcriptional activation domain into the nucleus, dictating the expression of genes for cholesterol biosynthesis, such as *HMGCR* and *SREBF2*, and the cholesterol uptake gene *LDLR* (*8*). Zebrafish genes *srebf1* and *srebf2* encode Srebp1 and Srebp2, respectively. Srebp1 is primarily responsible for fatty acid synthesis (*8*). We generated an *hsp70:Gal4ER*^{T2}*; UAS:apoa1bp2- 2A-mCerulean3* double transgenic animal, which expressed untagged Aibp2 upon heat shock with the addition of 4-hydroxy-tamoxifen (4OHT) (Fig. 2A and fig. S8, A and B). Srebp2 binds its own promoter and up-regulates its mRNA expression (*8*), which mirrors its transcriptional activity. Aibp2 deficiency reduced, and 4OHT-induced Aibp2 overexpression increased, *srebf2* expression, whereas *srebf1* expression was unchanged (Fig. 2, B and C, and fig. S8C). These results suggest that Aibp2 regulates Srebp2 activity.

We also explored the hypercholesterolemia effect on embryonic hematopoiesis. Adult female

[1]Center for Cardiovascular Regeneration, Houston Methodist, 6550 Fannin Street, Houston, TX 77030, USA. [2]Center for Bioinformatics and Computational Biology, Department of Cardiovascular Sciences, Houston Methodist, 6550 Fannin Street, Houston, TX 77030, USA. [3]Department of Geriatric Medicine, Xiangya Hospital, Central South University, Changsha, Hunan, P.R. China. [4]Department of Biochemistry and Molecular Biology, UTHealth McGovern Medical School, University of Texas MD Anderson Cancer Center and UTHealth Houston, Houston, TX 77030, USA. [5]Graduate School of Biomedical Sciences, University of Texas MD Anderson Cancer Center and UTHealth Houston, Houston, TX 77030, USA. [6]Department of BioSciences, Rice University, Houston, TX 77005, USA. [7]Children's Regenerative Medicine Program, Department of Pediatric Surgery, Center for Stem Cell and Regenerative Medicine, The Brown Foundation Institute of Molecular Medicine, University of Texas Health Science Center at Houston, Houston, TX 77030, USA. [8]Department of Medicine, University of California, San Diego, La Jolla, CA 92093, USA. [9]Division of Biological Sciences, Department of Cellular and Molecular Medicine, University of California, San Diego, La Jolla, CA 92093, USA. [10]Houston Methodist Institute for Academic Medicine, Houston Methodist Research Institute, Houston Methodist, 6550 Fannin Street, Houston, TX 77030, USA. [11]Department of Cardiothoracic Surgeries, Weill Cornell Medical College, Cornell University, Ithaca, NY 10065, USA. [12]Stem Cell Program and Division of Hematology/Oncology, Boston Children's Hospital and Dana-Farber Cancer Institute, Howard Hughes Medical Institute, Harvard Stem Cell Institute, Harvard Medical School, Boston, MA 02115, USA. [13]Department of Obstetrics and Gynecology, Houston Methodist, 6550 Fannin Street, Houston, TX 77030, USA.

*These authors contributed equally to this work.

†Corresponding author. Email: lhfang@houstonmethodist.org (L.F.); kchen2@houstonmethodist.org (K.C.); baiyongping@csu.edu.cn (Y.B.)

cmyb:GFP zebrafish fed a high-cholesterol diet (HCD) produced embryos with significantly higher cholesterol contents (fig. S9, A and B) and greater *srebf2* expression (fig. S9C). The embryos produced by the HCD-fed females showed more *cmyb*$^{+}$*kdrl*$^{+}$ HSCs than the embryos produced by females fed a control diet (fig. S9, D and E). Similarly, hypercholesterolemic female mice produce embryonic day 11.5 embryos with increased frequency of c-Kit^{+}CD144^{+}CD45.2^{-}- and RUNX1-enriched hemogenic ECs (HECs) and hematopoietic precursors (fig. S9, F to K). The data suggest that plasma cholesterol content regulates the developmental HSC program.

Cellular cholesterol homeostasis is sustained by low-density lipoprotein (LDL) cholesterol uptake, Srebp2-mediated cholesterol synthesis, and high-density lipoprotein (HDL)–mediated cholesterol efflux. Because cholesterol pools in the plasma membrane and ER are interconnected (*9*), we next probed the effect of cholesterol efflux on Srebp2 activation. Cholesterol sequestrant methyl-β-cyclodextrin robustly activated SREBP2 in human umbilical vein ECs (HUVECs) (fig. S8, D and E). AIBP augments the capacity of HDL to accept cholesterol (*5*), and AIBP and HDL combinatorial treatment dose-dependently activated SREBP2 (Fig. 2D and fig. S8F). These results suggest that Aibp2-mediated cholesterol efflux activates SREBP2. We hypothesized that Srebp2 mediates the Aibp2 effect on hematopoiesis. We thus generated *srebf2*$^{-/-}$ zebrafish (fig. S10, A to D). Srebp2 disruption markedly decreased *runx1*, *cmyb*, and *rag1* expression (Fig. 3A and fig. S11A) but did not influence *efnb2a* expression (Fig. 3A). Similarly, Srebp2 knockdown disrupted HSC emergence but showed no effect on DA specification, and the hematopoiesis defect was rescued by *srebf2* overexpression (fig. S12, A and B). Srebp2 knockdown markedly reduced the *cmyb*$^{+}$*kdrl*$^{+}$ HSCs (fig. S12, C and D) but had no effect on the formation of adjacent supporting tissues, shh signaling, and arterial and venous vessel specification (fig. S6, A and B), whereas it mildly increased the expression of pan-endothelial markers (fig. S6C). Srebp2 depletion specifically reduced the expression of Srebp2 but not Srebp1 downstream target genes (fig. S12E). These phenotypes support our hypothesis that Aibp2, through Srebp2 activation, controls HSC emergence. To test this, we created a *kdrl:Gal4ER*^{T2}*; UAS:Flag-nSrebp2-2A-mCerulean3* transgenic animal, in which the addition of 4OHT induced EC-specific transcriptionally active nuclear Srebp2 (nSrebp2) expression (*10*) (fig. S11, B and C). Nuclear *srebf2* mRNA injection into Aibp2 knockouts (Fig. 3B and fig. S13A) or 4OHT treatment of Aibp2-deficient *kdrl:Gal4ER*^{T2}*; UAS:Flag-nSrebp2-2A-mCerulean3* animals rescued impaired HSC emergence (fig. S11, D and E). Atorvastatin, which activates Srebp2 (*11*), markedly augmented *srebf2* but not *srebf1* expression (fig. S11F). Atorvastatin treatment augmented HSC emergence (fig. S13, C and D), which was abolished by Srebp2 disruption (Fig. 3C and fig. S13, B to D). Atorvastatin-enhanced HSC emergence is not due to HSC hyperproliferation, because similar numbers of bromodeoxyuridine-positive *cmyb*$^{+}$ cells in the DA were found in control and atorvastatin-treated animals at 30 and 36 hpf (fig. S14, A and B). Collectively, these findings suggest that Srebp2 acts downstream of Aibp2 to orchestrate HSC specification.

The key role of Notch in HSC specification prompted us to explore the role of Srebp2 in Notch signaling (*12*). We used a *tp1:d2GFP* Notch reporter zebrafish, which expresses a green fluorescent protein variant with a shortened half-life under the control of tandem Notch-responsive elements (*13*). The ablation of Aibp2 substantially reduced *tp1*$^{+}$*kdrl*$^{+}$ HSPCs, an effect that could be reversed by Aibp2 overexpression (fig. S15, A and B). Similarly, Srebp2 depletion decreased, whereas enforced nSrebp2 expression restored, *tp1*$^{+}$*kdrl*$^{+}$ HSPCs in the ventral DA (fig. S15, A and B). Furthermore, nSrebp2 overexpression rescued HSPC emergence in *apoa1bp2* morphants (fig. S15, A and B), indicating that Srebp2 mediates the Aibp2 effect on Notch signaling.

Aibp2 or Srebp2 deficiency markedly reduced the expression of *notch1b* but not that of *notch1a*, *notch2*, or *notch3* in the DA (Fig. 4A

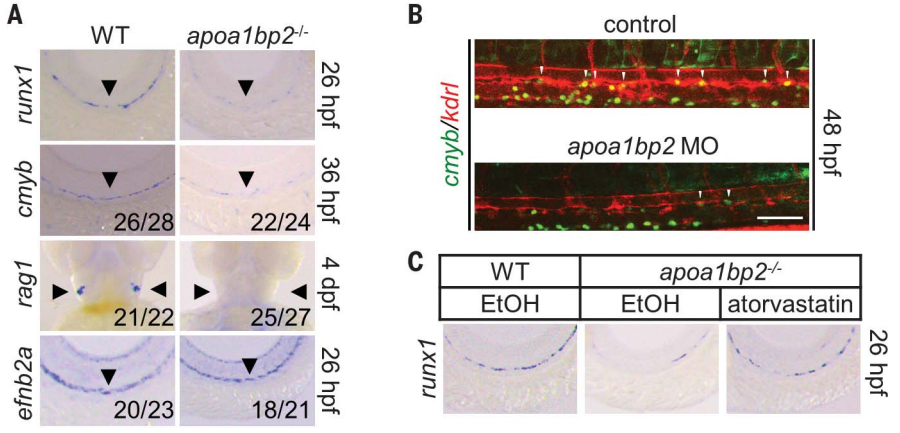

Fig. 1. Effect of Aibp2 and cholesterol on HSC emergence. (**A**) Whole-mount in situ hybridization (WISH) analysis of *runx1*, *cmyb*, *rag1*, and *efnb2a* expression. The numerator indicates the number of zebrafish with the representative phenotype, and the denominator indicates the total number of animals assessed. WT, wild type; dpf, days postfertilization. (**B**) HSC emergence in control or Aibp2-deficient *cmyb:GFP; kdrl:mCherry* zebrafish. (**C**) WISH analysis of *runx1* in animals with the indicated treatments. EtOH, ethanol. Arrowheads in (A) indicate the DA or thymus, and those in (B) show *cmyb*$^{+}$*kdrl*$^{+}$ HSCs. Scale bar, 100 μm.

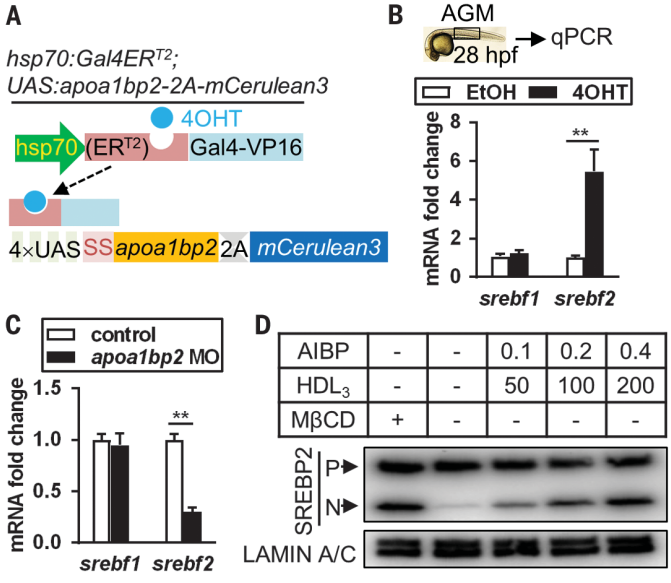

Fig. 2. Effect of Aibp2 on Srebp2 activity in ECs. (**A**) DNA constructs used to make the transgenic zebrafish with heat shock–induced Aibp2 expression. SS, secretion signal. (**B** and **C**) Quantitative reverse transcription PCR (qPCR) analyses of *srebf1* and *srebf2* in the aorta-gonad-mesonephros (AGM) regions of Aibp2 overexpression (B) or knockdown (C) zebrafish. MO, Morpholino antisense oligonucleotides. (**D**) Immunoblots of Srebp2 in HUVECs incubated with or without AIBP and HDL_3 (in micrograms per milliliter) for 4 hours. $^{**}P < 0.01$. MβCD, methyl-β-cyclodextrin; P, Srebp2 precursor; N, nSrebp2.

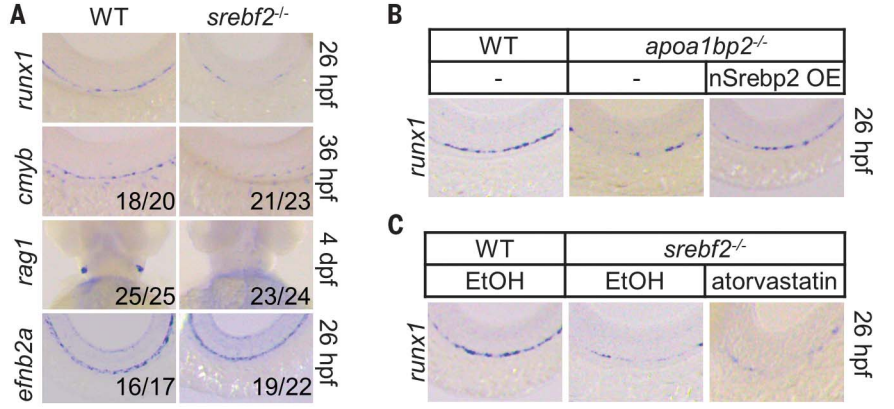

Fig. 3. Effect of Srebp2 on HSC emergence. (**A**) WISH analysis of the indicated genes in wild-type (WT) or *srebf2*$^{-/-}$ zebrafish. The numerator indicates the number of zebrafish with the representative phenotype, and the denominator indicates the total number of animals assessed. (**B** and **C**) WISH analysis of *runx1* expression in the DA. OE, overexpression.

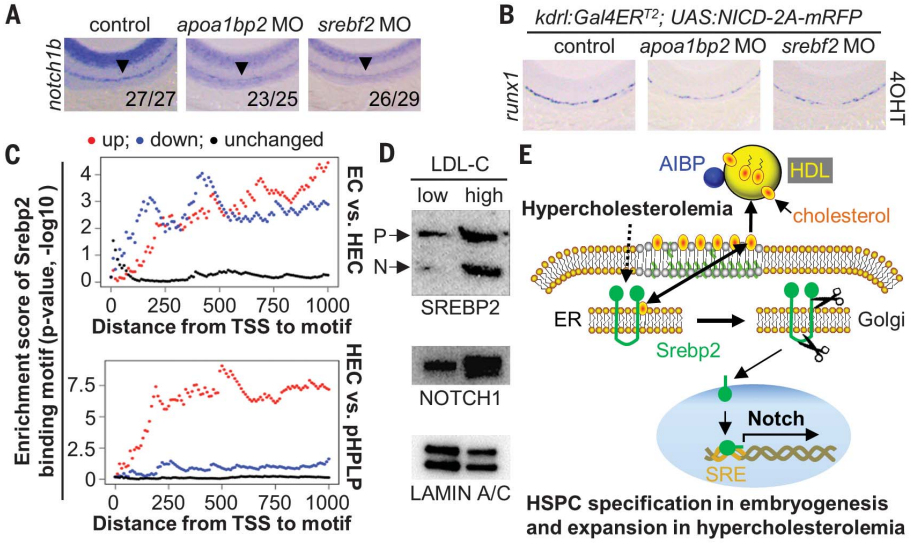

Fig. 4. Effect of AIBP-regulated Srebp2 activity on Notch signaling. (**A** and **B**) WISH analysis of *notch1b* and *runx1*. The numerator indicates the number of zebrafish with the representative phenotype, and the denominator indicates the total number of animals assessed. (**C**) Srebp2 binding motif enrichment in differentially expressed gene groups. TSS, translation start site. (**D**) Immunoblotting of SREBP2 and NOTCH1 in HSPCs isolated from subjects with low LDL cholesterol (LDL-C) (1.826 ± 0.089 mM; n = 5 subjects) and high LDL-C (4.796 ± 0.454 mM; n = 5 subjects). LAMIN A/C serves as the loading control. P, Srebp2 precursor; N, nSrebp2. (**E**) Working model. Bilateral cholesterol transport occurs between the ER and plasma membrane. AIBP-accelerated cholesterol efflux to HDL or hypercholesterolemia activates Srebp2, which transactivates Notch for hematopoiesis. SRE, sterol response elements.

and fig. S15C), suggesting that attenuated Notch signaling caused impaired HSC emergence in *apoa1bp2* or *srebf2* morphants. To investigate this possibility, *kdrl:Gal4ER*^{T2}*; UAS:NICD-2A-mRFP* transgenic animals that selectively express the 4OHT-inducible endothelial Notch intracellular domain (NICD) were created (fig. S15D). NICD expression restored *runx1* mRNA expression in *apoa1bp2*- or *srebf2*-deficient animals (Fig. 4B and fig. S15, E and F). Our findings agree with other findings that *notch1* is intrinsically required for HSC fate (*14*–*16*).

The *notch1b* promoter contains putative Srebp2 binding motifs, which was validated by chromatin immunoprecipitation (ChIP) coupled with quantitative polymerase chain reaction (ChIP-qPCR) analyses of the targeted region (fig. S16, A and B). By analyzing data from ChIP with sequencing (ChIP-seq) for mouse Srebp2 (*17*), we found a prominent Srebp2 binding peak in the promoters of *Notch1* (fig. S16C) and validated the Srebp2 binding (fig. S17B).

Furthermore, we performed a bioinformatics scan of the whole mouse genome by using the putative Srebp2 binding motif, which is enriched at the center of Srebp2 ChIP-seq peaks (fig. S16D). Our results indicate that the Srebp2 binding motif is highly enriched in the promoters of genes for cholesterol metabolism and Notch signaling (fig. S16E and tables S1 and S2), suggesting that this motif is highly conserved. For example, the Srebp2 binding motif and ChIP-seq peak are present in the promoters of Srebp2-regulated cholesterol biosynthesis genes *Srebf2*, *Hmgcr*, and *Ldlr* (fig. S17A), all of which were experimentally verified in murine ECs with Srebp2 overexpression (fig. S17, B and C). Furthermore, Srebp2 ChIP-seq results (*17*) also validated Srebp2-mediated regulation of Notch signaling and cholesterol metabolism (fig. S18, A and B).

To further investigate the role of Srebp2 in hematopoiesis, we compared gene expression profiles in paired murine ECs, a Ly6a–green fluorescent protein–positive population that contains HECs, and pre-HSCs and progenitors with lymphoid potential (pHPLPs) (*18*). Compared with ECs, HECs had 752 genes up-regulated and 569 genes down-regulated, whereas compared with HECs, pHPLPs had 752 genes increased and 977 genes decreased (fig. S19A). Notch pathway genes are substantially enriched among the genes up-regulated in HECs compared with ECs or pHPLPs (table S3 and fig. S19B). Except for *Scap*, most Srebp2-regulated cholesterol metabolism genes were repressed in HECs (table S3). SCAP is a protein chaperone of Srebp2 and is retained in the ER membrane by sterol-induced interaction with ER-resident protein INSIG1/2 (*8*). *Scap* expression increased by up to fourfold in HECs compared with ECs (table S3). The Srebp2 binding motif or ChIP peak is markedly enriched in the promoters of up-regulated genes, but to a lesser extent in the promoters of down-regulated genes (Fig. 4C and fig. S18C). Consistent with this, our results from an assay for transposase-accessible chromatin using sequencing (ATAC-seq) unveiled that the Srebp2 binding motif and ChIP-seq peak are located within active transcription–associated open chromatin regions of HECs, with 42% of binding motifs (fig. S16, F and G) and 79% of ChIP-seq peaks (fig. S18, D and E) overlapping the ATAC-seq peaks in HECs. Thus, our systemic bioinformatics analyses independently validate our findings that Srebp2 is a critical regulator of the Notch pathway.

We further explored the effect of hypercholesterolemia on adult hematopoiesis. As reported previously (*19*, *20*), Western diet (WD) feeding augmented HSPC frequency in *Ldlr*$^{-/-}$ mice, and Srebp2 suppression by betulin abolished the WD-induced augmentation of HSPC frequency (fig. S20, A to C). To relate our findings to human disease, we assessed the circulating $CD34^{+}CD45^{+}$ HSPCs in healthy volunteers. We found that LDL cholesterol levels are correlated with HSPC frequency (fig. S20D) and that Srebp2 is activated and Notch is up-regulated

in HSPCs isolated from hypercholesterolemic subjects (Fig. 4D and table S4). Collectively, our data document a conserved Srebp2-dependent mechanism that regulates HSPC maintenance in hypercholesterolemia.

Accumulating studies indicate that Srebp2 has moonlighting activities (*17*, *21*). We showed that the somite-derived prohematopoietic Aibp2 controls hematopoiesis by targeting Srebp2-regulated cholesterol metabolism and Notch signaling (Fig. 4E). In murine HECs, only the cholesterogenic gene *Scap* is significantly up-regulated. Given that SCAP gain of function increases sterol-independent Srebp2 bioavailability (*22*), SCAP up-regulation may contribute to increased Srebp2 activation in HECs. The Srebp2 function in HECs may be shifted more toward Notch activation than cholesterol regulation. Our findings also corroborate the essential role of the somite in providing proper Notch signaling for HSC specification; for example, Wnt16-induced Dlc/Dld presented by the sclerotome regulates Notch1b activity in the migrating HSC precursors (*23*, *24*).

Hypercholesterolemia is the driving force for atherosclerosis that underlies heart attacks and strokes. Hypercholesterolemia activates endothelial Srebp2 (*8*, *21*). Srebp2 activation and Notch1 up-regulation are detected in circulating HSPCs of hypercholesterolemic human subjects. Srebp2-regulated Notch1 signaling may also orchestrate HSPC homeostasis in hypercholesterolemia. It appears that both AIBP-mediated cholesterol efflux and hypercholesterolemia converge on endothelial Srebp2 activation. Taking these findings together, we have uncovered a cholesterol metabolism pathway governing HSPC emergence in development as well as HSPC expansion in hypercholesterolemia. These insights may have relevance for hematological and cardiovascular disorders.

REFERENCES AND NOTES

1. J. Y. Bertrand *et al*., *Nature* **464**, 108–111 (2010).
2. J. C. Boisset *et al*., *Nature* **464**, 116–120 (2010).
3. K. Kissa, P. Herbomel, *Nature* **464**, 112–115 (2010).
4. P. D. Nguyen *et al*., *Nature* **512**, 314–318 (2014).
5. L. Fang *et al*., *Nature* **498**, 118–122 (2013).
6. N. D. Lawson *et al*., *Development* **128**, 3675–3683 (2001).
7. T. E. North *et al*., *Cell* **137**, 736–748 (2009).
8. M. S. Brown, J. L. Goldstein, *Cell* **89**, 331–340 (1997).
9. A. Das, M. S. Brown, D. D. Anderson, J. L. Goldstein, A. Radhakrishnan, *eLife* **3**, e02882 (2014).
10. S.-W. Jin, D. Beis, T. Mitchell, J.-N. Chen, D. Y. Stainier, *Development* **132**, 5199–5209 (2005).
11. M. S. Brown, J. L. Goldstein, *Proc. Natl. Acad. Sci. U.S.A.* **96**, 11041–11048 (1999).
12. E. Butko, C. Pouget, D. Traver, *Dev. Biol.* **409**, 129–138 (2016).
13. B. S. Clark *et al*., *Development* **139**, 1599–1610 (2012).
14. B. K. Hadland *et al*., *Blood* **104**, 3097–3105 (2004).
15. K. Kumano *et al*., *Immunity* **18**, 699–711 (2003).
16. A. D. Kim *et al*., *EMBO J.* **33**, 2363–2373 (2014).
17. Y. K. Seo *et al*., *Cell Metab.* **13**, 367–375 (2011).
18. P. Solaimani Kartalaei *et al*., *J. Exp. Med.* **212**, 93–106 (2015).
19. A. J. Murphy *et al*., *J. Clin. Invest.* **121**, 4138–4149 (2011).
20. M. Westerterp *et al*., *Cell Stem Cell* **11**, 195–206 (2012).
21. Z. Chen *et al*., *Circulation* **131**, 805–814 (2015).
22. J. D. Horton *et al*., *Proc. Natl. Acad. Sci. U.S.A.* **100**, 12027–12032 (2003).
23. W. K. Clements *et al*., *Nature* **474**, 220–224 (2011).
24. I. Kobayashi *et al*., *Nature* **512**, 319–323 (2014).

ACKNOWLEDGMENTS

We thank the Brown and Goldstein lab (UTSW), T. Osborne (SBP), S. Gerety (WTSI), and B. Link (MCW) for providing antibodies, DNA constructs, or transgenic zebrafish. We thank C. Liu (UCSD) and H. Wu's lab (BCM) for technical support. We thank I. Slukvin (UW), B. Zhou (SIBCB), and M. Yoshimoto (UTH) for helpful discussions. **Funding:** The project was supported by grants to L.F. from the National Heart, Lung, and Blood Institute (HL114734 and HL132155) and the American Heart Association (16BGIA27790081 and 18TPA34250009); to L.I.Z. from the National Institutes of Health (HL04880 and DK49216); to P.L.W. from the National Institutes of Health (K01DK092365 and R01DK111599) and the Cancer Prevention and Research Institute of Texas (RP110776); to Y.I.M. from the National Heart, Lung, and Blood Institute (HL135737); to W.L. from the Cancer Prevention and Research Institute of Texas (RR160083) and the National Institutes of Health (CA204468); to J.P.C. and K.C. from the National Heart, Lung, and Blood Institute (HL133254); to K.C. from the National Institutes of Health (GM125632) and the Cancer Prevention and Research Institute of Texas (RP120348 and RP170002); and to X.Y. from the American Heart Association (17POST33410671). **Author contributions:** Q.G. and L.F. conceived the project, designed the experiments, and wrote the manuscript. L.F. supervised the project. Q.G. performed the majority of the experiments and analyzed the data. X.Y., J.K., S.M., T.P.C., B.T., D.S.W., and M.F.D. performed experiments and/or offered research assistance. J.L., B.X., and K.C. contributed to RNA-seq, ChIP-seq, and ATAC-seq data analyses. J.Z. and Y.B. contributed to human blood collection and data analysis. R.W. and F.X. contributed to ATAC-seq library generation and sequencing. L.I.Z., D.T., J.P.C., and P.L.W. provided constructive suggestions and experimental materials. D.S.W., P.L.W., W.L., Y.I.M., D.T., J.P.C., L.I.Z., K.C., Y.B., and L.F. critically revised the manuscript. **Competing interests:** Y.I.M. and L.F. are inventors on a patent and patent application (US20160115211A1 and WO2014193822A1) submitted by The Regents of The University of California that covers compositions and methods for regulating angiogenesis and cholesterol and treating dyslipidemia, atherosclerosis, cancer, and inflammatory conditions. L.I.Z. holds stock in, is a consultant to, and is on the scientific advisory board of FATE Therapeutics, Scholar Rock, Camp4, and Celularity. **Data and materials availability:** The ATAC-seq data of this study are deposited in the NCBI Gene Expression Omnibus (GEO) under accession number GSE122204.

SUPPLEMENTARY MATERIALS

www.sciencemag.org/content/363/6431/1085/suppl/DC1
Materials and Methods
Figs. S1 to S20
Tables S1 to S4
References (*25*–*45*)
Movies S1 and S2

21 August 2018; accepted 22 January 2019
Published online 31 January 2019
10.1126/science.aav1749

AIBP-mediated cholesterol efflux instructs hematopoietic stem and progenitor cell fate

Qilin Gu, Xiaojie Yang, Jie Lv, Jiaxiong Zhang, Bo Xia, Jun-dae Kim, Ruoyu Wang, Feng Xiong, Shu Meng, Thomas P. Clements, Bhavna Tandon, Daniel S. Wagner, Miguel F. Diaz, Pamela L. Wenzel, Yury I. Miller, David Traver, John P. Cooke, Wenbo Li, Leonard I. Zon, Kaifu Chen, Yongping Bai and Longhou Fang

Science **363** (6431), 1085-1088.
DOI: 10.1126/science.aav1749originally published online January 31, 2019

Regulating HSC progenitors via cholesterol

Atherosclerosis is characterized by the buildup of cholesterol-containing lipoproteins in the vascular wall. This increased cholesterol augments hematopoietic stem and progenitor cell (HSPC) counts, and the resultant increase in leukocytes is associated with increased cardiovascular disease. Gu *et al.* describe a mechanism orchestrating HSPC specification from the hemogenic endothelium (HE) during embryogenesis (see the Perspective by Rajan and Berman). ApoA-I binding protein accelerated cholesterol efflux from the HE, activating the transcription factor Srebp2, which in turn transactivated Notch signaling. This mechanism also appears to be important for adult HSPC expansion in hypercholesterolemia.

Science, this issue p. 1085; see also p. 1041

Science (print ISSN 0036-8075; online ISSN 1095-9203) is published by the American Association for the Advancement of Science, 1200 New York Avenue NW, Washington, DC 20005. The title *Science* is a registered trademark of AAAS.